

XMET: A XENON ELECTROTHERMAL THRUSTER USING ADDITIVE MANUFACTURING

SPACE PROPULSION 2018
BARCELO RENACIMIENTO HOTEL, SEVILLE, SPAIN / 14 – 18 MAY 2018

D. Staab⁽¹⁾, A. Frey⁽¹⁾, A. Garbayo⁽¹⁾, L. Shadbolt⁽¹⁾, A. Grubisic⁽²⁾, D. Hoffman⁽²⁾, F. Romei⁽²⁾, D. Faircloth⁽³⁾, S. Lawrie⁽³⁾

⁽¹⁾ AVS UK Ltd - Rutherford Appleton Laboratory, Chilton, (United Kingdom), Email: dstaab@a-v-s.uk.com

⁽²⁾ University of Southampton, Southampton (United Kingdom)

⁽³⁾ STFC ISIS Spallation Neutron and Muon Facility, Rutherford Appleton Laboratory, Chilton, UK

KEYWORDS: electrothermal thrusters, electric propulsion, microwave, xenon, all-electric

ABSTRACT:

This work presents XMET, a Xenon Microwave Electro-thermal Thruster. XMET uses a free-floating plasma discharge in a cylindrical resonant cavity operating at 2.45 GHz. It will be used as the RCS thruster for an integrated propulsion architecture for small GEO platforms, sharing common propellant and power systems with a gridded ion engine. We discuss the theoretical background of METs, previous work in the field and describe resonant cavity modelling and optimisation done for XMET. The XMET prototype design is explained, including the use of exchangeable nozzle insets produced in additive manufacturing. XMET is currently undergoing testing, including direct thrust measurements.

1. BACKGROUND AND MOTIVATION

The Integrated Microwave Propulsion Architecture for Telecommunication Satellites (IMPULSE) project aims to develop a highly innovative propulsion architecture for a new generation of all-electric small geostationary (GEO) platforms. The consortium is led by the University of Southampton and includes AVS UK and the STFC-ISIS group. IMPULSE will enable GEO spacecraft with fully all-electric propulsion for station keeping, orbit raising, and the reaction control system (RCS). “Fully all-electric” here refers to the concept of a highly integrated primary and secondary RCS propulsion system, operating on a common propellant and power architecture (c.f. [1]). This reduces propulsion system mass, cost and complexity and completely eliminates the use of hydrazine, a key operational and safety benefit. IMPULSE uses a primary Gridded Ion Engine (GIE) exploiting microwave-based electron cyclotron resonance, in combination with microwave electro-thermal thrusters (MET) for the RCS. The GIE and MET use the same 2.45 GHz microwave generator and

xenon propellant. This concept originated at the University of Southampton, and will be fully described in a forthcoming publication. The current paper will only discuss the design of the Xenon Microwave Electro-Thermal thruster (XMET) itself.

2. PREVIOUS WORK

The basic operating principle of METs is the use of microwaves (mw) to create a free-floating plasma discharge in a cylindrical cavity resonator, which can efficiently heat a wide range of gaseous propellants. The propellant is then expanded through a conventional gas dynamic nozzle. METs have been developed in the US over the last decades, with the design evolving towards simple, rugged thrusters that are inexpensive, highly scalable and compatible with a wide range of propellants. The free-floating plasma discharge avoids erosion of crucial components and no cathodes are required for either plasma generation or exhaust neutralisation. This makes METs a plausible competitor to resistojets and arcjets (at similar thrust levels), since these are limited by thermal endurance of the resistive heating element and cathode erosion respectively. Note METs have not been flown to date. A set of laboratory prototypes with cavity radii of 50-7 mm have been tested using frequencies of 2.45-17.8 GHz, power levels of ~ 2000-20 W, and thrust levels of ~ 300-1mN ([2], [3] and references therein). The vast majority of this work has been carried out at Penn State university. After initial tests of a non-optimised 2.45 GHz prototype, this programme has focussed on small satellite propulsion applications by using higher frequency, smaller, low power, low thrust devices. Propellants studied to date including nitrogen, oxygen, helium and argon - promising specific impulse (I_{sp}) of 500 and 800 seconds was achieved with ammonia and water respectively ([4],[3]). Recently, the Bogazici University Space Technologies Laboratory (BUSTLab) has begun testing of a more optimised 2.45 GHz prototype similar to the Penn State

design [5]. Note that our use of Xenon propellant due to the overall IMPULSE architecture limits the achievable XMET specific impulse compared to propellants with lower molecular weight. We are not aware of any published Xenon MET results to date. An important benchmark for XMET is to significantly exceed the I_{sp} of Xenon resistojets such as the SSTL T-30 [6] by achieving higher chamber temperatures. A comparison of this thruster, the most recent 2.45GHz MET performance data published and the performance goals for XMET is given in Tab.1.

Table 1: Comparison of our XMET performance goals with an operational resistojet and recent MET prototype results.

thruster	propellant	thrust [mN]	I_{sp} [s]	power [W]
SSTL T-30 [6]	xenon	~100	48	30
MET BUSTLab [5]	argon	200-350	80-100	< 200
XMET	xenon	200 -500	100	< 1000

3. MET RESONANT CAVITY THEORY

Establishing a useful, stable plasma discharge with good heat transfer to the propellant requires a resonant cavity mode where the electric field strength peaks directly at the nozzle inlet. For this reason, the so-called transverse magnetic $TM^{z_{011}}$ mode is used in all METs developed following the work in [7]. In most designs, the geometry and field are symmetric, i.e. also peaking at the antenna end of the cavity. The antenna is protected from plasma formation and erosion via a dielectric plate at the cavity mid-plane, preventing propellant from reaching the antenna. As discussed in [8], an alternative is loading the cavity with a dielectric disk aligned with the antenna cavity end, resulting in an axially asymmetric electric field distribution: its strength is decreased near the dielectric, and increased near the nozzle.

The $TM^{z_{011}}$ mode of an empty cylindrical cavity with perfectly conducting walls has a resonant frequency f_{res} governed by cavity height h_c and internal radius a :

$$f_{res} = \frac{1}{2\pi\sqrt{\mu_0\epsilon_0}} \sqrt{\left(\frac{\chi_{01}}{a}\right)^2 + \left(\frac{\pi}{h_c}\right)^2}, \quad (1)$$

where ϵ_0 and μ_0 are the permittivity and permeability of free space, and $\chi_{01} = 2.4048$ is a zero of the Bessel function. At a constant radius, f_{res} initially drops rapidly with increasing h_c and then asymptotes to a minimum value. The ratio between electric field strengths at the nozzle end and mid-plane of the cavity is linearly proportional to h_c/a , therefore larger h_c/a ratios are desirable.

Ratios of around 3 have been successfully used in the Penn State prototypes [2]. For XMET, resonance must be achieved at 2.45 GHz. Rearranging Equation 1, we can see this imposes a minimum cavity radius: regardless of h_c , there are no solutions for $a < 47$ mm. In the case of a cavity including a dielectric disk (with thickness t_s and radius a equal to that of the cavity), the following relations between the z-direction wavenumbers in the dielectric and vacuum domains (β_d and β_{vac}) must hold.

$$\frac{\beta_d}{\epsilon_d} \tan(\beta_d t_s) = \frac{\beta_{vac}}{\epsilon_0} \tan[\beta_{vac}(t_s - h_c)], \quad (2)$$

$$\beta_d = \sqrt{\omega^2 \mu_d \mu_0 \epsilon_d \epsilon_0 - \left(\frac{\chi_{01}}{a}\right)^2}, \quad (3)$$

$$\beta_{vac} = \sqrt{\omega^2 \mu_0 \epsilon_0 - \left(\frac{\chi_{01}}{a}\right)^2}, \quad (4)$$

where $\omega = 2\pi f_{res}$ and ϵ_d and μ_d are the relative permeability and permittivity of the dielectric material used. Derivations of Equations 1-4 can be found in e.g. [2]. These equations show that the minimum cavity radius for a given frequency is unaffected by the dielectric.

To optimise a given cavity design, the frequency and sharpness (FWHM) of its resonance are the key metrics and the fundamental task is to maximise the electric field strength at the nozzle throat. This will lead to the highest gas temperatures and thruster performance. The influence of parameters such as the dielectric position, antenna size and protrusion depth on the field strength should be investigated. For this type of work, numerical modelling of the cavity via multiphysics software is ideal and was used initially by [2]. The analysis showed that the 2.45 GHz cavity as constructed was significantly off-resonance. Subsequent METs were optimised via modelling before construction. In our work, we used the analytical relations given above to constrain the parameter space of interest for the modelling described in Section 4.

4. RESONANT CAVITY MODELLING AND DESIGN

The geometry of the model we used was set up as in [2] and is defined by Fig.1. The coaxial port and its antenna that feeds the microwave input to the cavity is included in the model. Cavity walls and antenna surfaces are approximated as perfect electric conductors and all domains not occupied by dielectrics are treated as vacuum. Cavity excitation is implemented via a coaxial port boundary condition. The coordinate system is cylindrical - only positive z and r coordinates are relevant due to symmetry. The model output of greatest interest is the maximum electric field strength in the plasma section of the cavity. In all

basic models, this is located at $z = h_c + h_p$, $r = 0$ (Fig.1), and will be referred to hereafter as $|E_{max}|$. We benchmarked our model by reproducing results reported in [2] and [9], and verified that sufficient mesh elements were used.

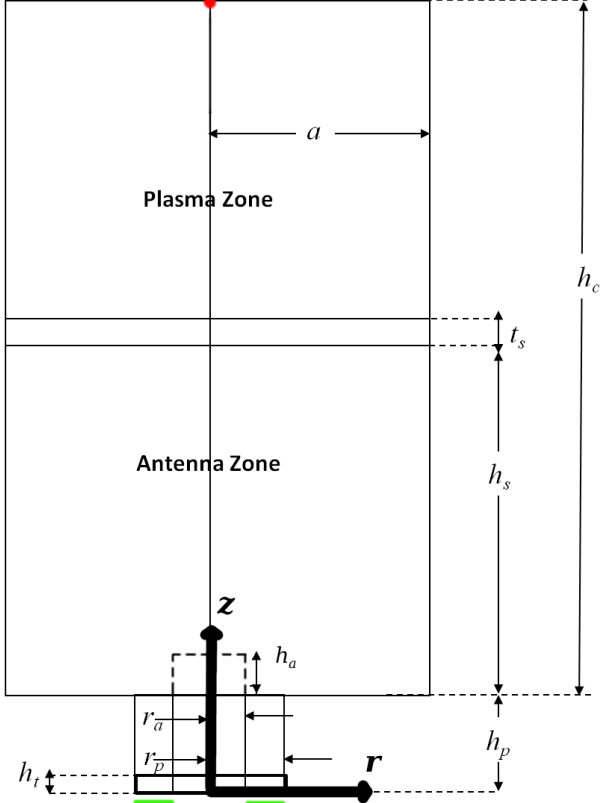


Figure 1: Geometry used in our modelling. The point with maximum electric field strength in the plasma section for the TM_{011}^z resonance mode is highlighted (red). Note this is the location of the nozzle, which is not included in this basic model. The surface where the port boundary condition is applied is highlighted in green.

4.1 Dielectric material options

The two dielectric materials considered were Boron Nitride (BN) and Alumina (Al_2O_3 , also known as Corundum). They are the most refractory dielectrics in widespread use, and highly resistant to erosion by Xenon ion bombardment (e.g. [10]). Boron Nitride has extensive electric propulsion flight heritage in Hall Effect thrusters. Both have similar maximum recommended use temperatures of ~ 2300 K and good resistance to thermal shocks. The primary difference of interest for cavity design is their permittivity, ranging from 8.5-9.9 for Al_2O_3 to 3.8-4.6 for BN, depending on the grade of material used. For initial comparative analysis, we used $\epsilon_{(Al_2O_3)} = 9.9$ and $\epsilon_{(BN)} = 4.2$. For final analysis and design, we chose the high purity, self-bonded BN (AX05) grade provided by Saint Gobain, with an isotropic permittivity of 4.0.

4.2 Optimisation of electric field strength

Note that the field strength in the cavity scales with the square root of input power P_{in} . We kept P_{in} and

the cavity radius fixed at 1kW and 50.8mm respectively, and explored the parameter space of possible cavity geometries, searching for the highest $|E_{max}|$ values. We used values of h_p , h_t , r_a and r_p consistent with a standard 7/16 coaxial panel mount connector with an M3 screw termination (c.f. Tab.2). The antenna consists of a small copper cylinder screwed onto this termination, producing a smooth surface with precise dimensions instead of the screw that would lead to dramatic local field enhancement effects. For practical values of the radius of this cylinder (r_a), very similar optimised resonance properties were observed in our modelling. We then fixed $r_a = 4.5$ mm. The main parameters affecting $|E_{max}|$ and the field strength distribution in the cavity are h_a , h_c , h_s and t_s . We tested a large number of permutations of these values, concluding that highest $|E_{max}|$ values are always achieved for $h_a = 0 = h_s$, i.e. antenna and dielectric flush with the bottom of the cavity. This asymmetric TM_{011}^z resonance option (see Section 3) always outperforms other geometries and will be used in our thruster prototype. All these conclusions hold for both Boron Nitride and Alumina. The key difference between dielectrics with significantly different permittivities is a dramatic change in resonance sharpness and peak $|E_{max}|$ as shown in Fig.2.

Table 2: Definitions of XMET resonant cavity variables (see Fig.1) and optimised values.

Variable	Value	Description
f_{res}	2.45 [GHz]	Resonant frequency
a	50.8 [mm]	cavity radius
h_c	103.5 [mm]	cavity height
t_s	14.5 [mm]	dielectric thickness
h_s	0 [mm]	separation antenna-dielectric
h_a	0 [mm]	antenna height in cavity
h_p	13 [mm]	coax. port height (outside cavity)
h_t	5 [mm]	height of teflon domain in coaxial port
r_p	8 [mm]	coax. port radius
r_a	4.5 [mm]	antenna radius
$\epsilon_{(BN)}$	4.0	permittivity of dielectric

For both dielectrics, there is a tight relationship between h_c and t_s along which resonance occurs with near-identical sharpness and peak $|E_{max}|$ values. Fig.2 illustrates that compared to the best-case Penn State 2.45 GHz prototype, $|E_{max}|$ at peak resonance is 8 and 42 times higher for our optimised Boron Nitride and Alumina geometries. The FWHM of the resonances are 12 MHz and 0.4 MHz respectively. The extreme sharpness of resonance for Alumina poses a key risk: off-resonance operation becomes highly likely, and tuning the cavity to maintain the high field strength would be much more difficult. Very tight manufacturing and material property tolerances and sensitivity to thermal expansion etc. would be problematic. With BN, the field strength is

significantly above the Penn State (prototype) level over a much broader frequency range, while still reaching an order of magnitude peak $|E_{max}|$ improvement. We therefore selected Boron Nitride as the XMET dielectric.

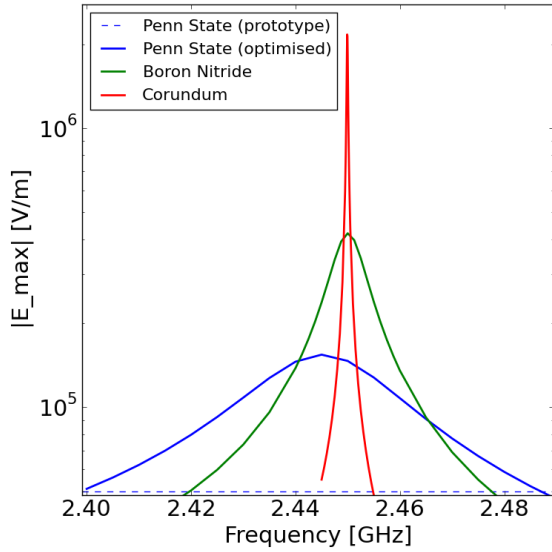


Figure 2: $|E_{max}|$ as a function of input frequency for Boron Nitride and Alumina dielectrics. For comparison, we show the resonance of the Penn State design as optimised by [9], and the best-case $|E_{max}|$ value at 2.45 GHz achieved in the actual Penn State prototype as built and tested ($\sim 0.5 \times 10^5$ V/m, [2]).

4.3 Cavity material, mass and size

Stainless 316 is an ideal material for the additive manufacturing that will be used for XMET, and has been successfully used in several previous METs. While Aluminium would allow mass savings, its lower maximum use temperature and increased sensitivity to plasma sputtering are of concern. As mentioned in the previous Section, many combinations of h_c and t_s achieve similar resonant cavity performance.

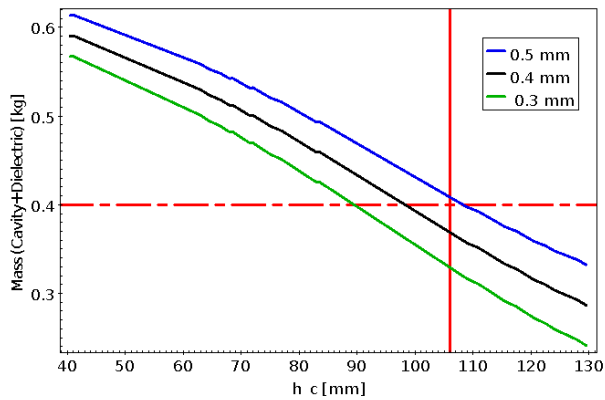


Figure 3: Illustration of XMET mass imposed by resonance condition as a function of cavity height for a radius of 50.8mm and uniform cylindrical wall thicknesses ranging from 0.3-0.5 mm. Electric field and system requirements impose $h_c < 105$ mm and mass < 0.4 kg (shown in red).

At resonance, the shorter t_s , the larger h_c , and the lower the total mass, since the dielectric slab dominates the cavity mass budget for the parameter space of interest (Fig.3), with the density of BN (grade AX05) and Stainless Steel (316) of 1.9 and 7.8 g/cm³ respectively.

In terms of mass, increasing the cavity height and decreasing dielectric thickness as much as possible is advantageous. However, a limit is imposed by the change in electric field distribution that occurs as the height continues to increase. We found that beyond $h_c \sim 105$ mm, the field strength directly at the top surface of the dielectric slab increases significantly. This risks plasma formation next to its surface, thermal damage to the dielectric, and potentially disruption of the desired plasma location directly at the nozzle inlet. The optimised preliminary cavity design we settled on was therefore $t_s = 14.5$ mm, $h_c = 104.5$ mm, with $|E_{max}| \sim 6 \times 10^5$ V/m (Fig.4). Note that holes in the cavity wall with diameter \ll the microwave wavelength at 2.45 GHz have no significant effect on either resonance properties or electric field distribution - this includes the propellant injector and nozzle orifices.

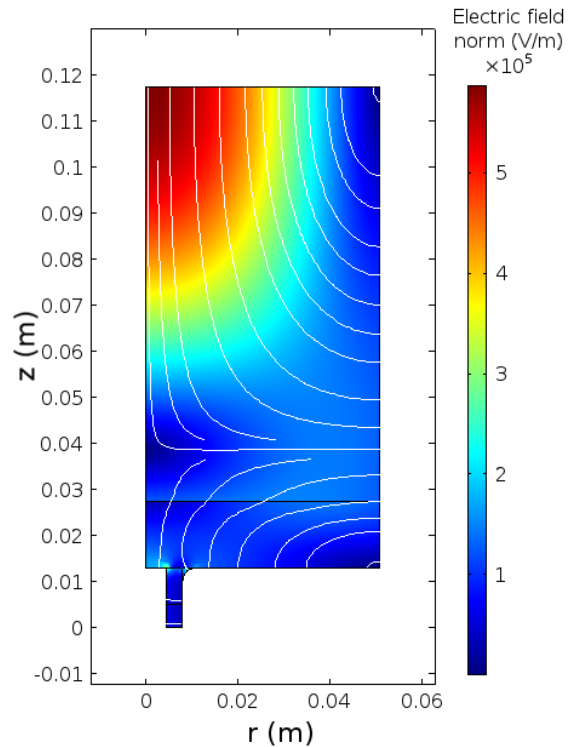


Figure 4: Electric field strength and streamlines at peak resonance ($P_{in} = 1$ kW) throughout the preliminary cavity geometry design. Half of the cavity is shown due to symmetry. The nozzle throat is located at the top left, where the field peaks.

4.4 Cavity tuning

A key risk for the project is that the MET prototype as built has a somewhat different resonant frequency compared to the model prediction of 2.45 GHz. Due to the relatively sharp resonance (even for Boron Nitride), this could lead to off-resonance operation with significantly worse

performance, or even prevent plasma ignition. To mitigate this risk, a tuneable prototype cavity design is highly desirable. This can be achieved since the cavity needs to be assembled in two pieces in any case - a base with the coaxial connector, antenna and dielectric slab, and the top part with the nozzle. We decided to connect these two parts via a simple thread and O-ring seal combination. Rotating the top against the bottom part changes the cavity height in a highly controlled way with small step sizes, thereby allowing tuning. After completion of prototype tests a fixed-format flight-like design will be implemented without this mechanical tuning capability. A microwave generator with tuneable frequency output across a small bandwidth around 2.45 GHz will likely be used instead.

We adapted the basic model to the geometry changes imposed by the two part threaded design, which modified the optimum predicted cavity height to 103.5 mm. Fig.5 shows how the resonance of this finalised model responds to changes in cavity height tuning, under the assumption that all other cavity parameters are exactly as given in Tab.2. Using this tuning capability we can therefore compensate for plausible deviations in cavity geometry (arising from manufacturing tolerances) and in variations from the nominal AX05 Boron Nitride permittivity. The latter, along with the cavity radius a are by far the most critical parameters for resonance.

With our threaded 2-part cavity design, we can adjust h_c in steps of 0.1 mm via rotating through 1/16th of a full turn. We therefore expect to be able to reach $|E_{max}| \sim 4 \times 10^5$ V/m with tuning (Fig.5) at the 1 kW power level. Since $|E_{max}|$ is proportional to $P_{in}^{0.5}$, ignition and steady-state operation with comparable cavity performance as for the Penn State 2.45 GHz prototype will be achieved at significantly lower power levels. At 1 kW, an order of magnitude improvement in $|E_{max}|$ is achieved with our design.

5. XMET DETAILED DESIGN

Separate from electromagnetic resonant cavity optimisation, an appropriate design for the flow control elements (nozzle and propellant injectors) is crucial for METs. Outflow is controlled by the nozzle, and the inflow and vortex flow pattern are controlled by the injectors. A complete, coupled EM-plasma-CFD modelling effort is beyond the scope of this work. Due to the dependence of the floating discharge behaviour on the operating pressure and the nozzle throat size such a complete treatment would be needed to select the optimal nozzle and injector design a priori. In previous MET development, a common approach taken is to avoid this complexity and to rely on experimental characterisation of different nozzle and injector sizes.

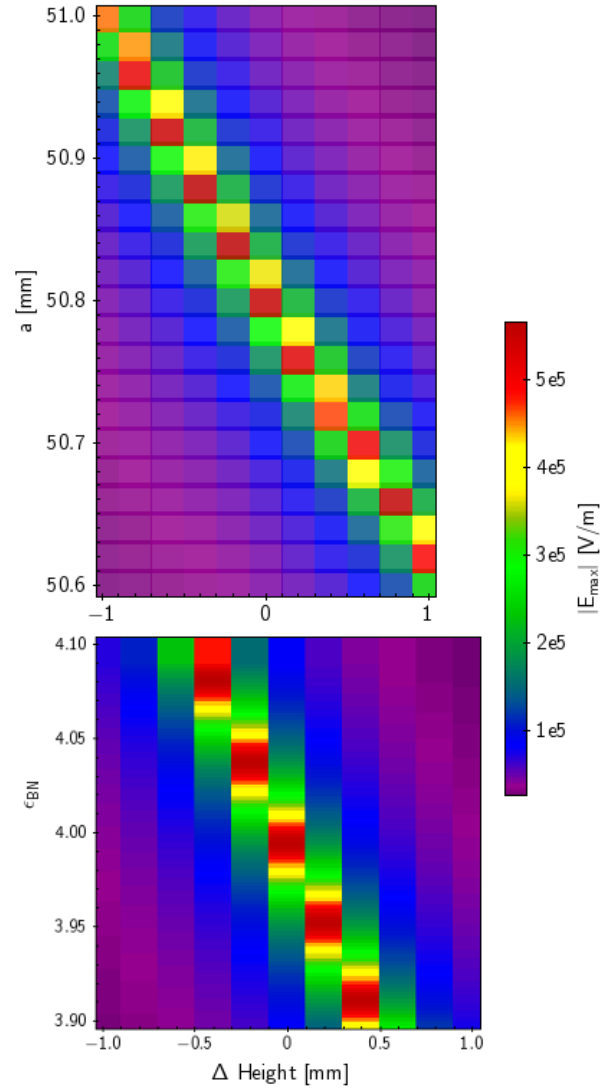


Figure 5: Peak electric field strength over a grid of simulations with different cavity height changes (tuning), for a range of cavity radii (top) and dielectric permittivities (bottom).

As described in [2], increasing the chamber pressure P_c will force the coalesced plasma discharge closer to the nozzle throat. This reduces cold flow slippage, i.e. the amount of propellant flow into the nozzle with reduced plasma heating. At even higher P_c values, the plasma is less stable, precessing about the cavity axis, and cold flow slippage increases again. The net effect is an optimum operating pressure for a given nozzle throat size, propellant, and power level; where specific impulse is maximised. We are using our XMET prototype to experimentally determine the optimum nozzle size and operating pressure.

5.1 Injectors

We are using the standard MET tangential injector configuration: two holes drilled at an exactly tangential angle into the cavity side walls, close to the nozzle end. These injection ports are fed by propellant lines splitting from a common supply.

Tangential injection creates a vortex flow pattern, cooling the cavity walls and stabilizing the central plasma region. The critical design parameter is the diameter of the injector orifices, d_i . Smaller d_i values increase the injection velocity, leading to better plasma stabilization and significantly improved performance [2]. The best solution is the smallest d_i value that still allows the maximum input mass flow rate desired during operations (given the upstream supply pressure). For our XMET prototype setup we estimated this is $d_i = 0.6\text{mm}$ for tests with both argon and xenon propellant.

5.2 Nozzle

We selected a simple nozzle design with a conical cross-section, area ratio of 200, divergence half-angle of 15 degrees, and a circular-contour converging section with radius 3mm. This is very similar to the SSTL T-50 xenon resistojet nozzle geometry, and could be optimised in future work. The primary goal in current testing is to find the optimal throat diameter (d^*), while keeping all other nozzle parameters listed above fixed. We therefore designed XMET with exchangeable nozzle insets, initially covering $d^* = 0.9\text{--}2.0\text{ mm}$ (Fig.6). Nozzle lengths and exit plane diameters scale accordingly. To reduce costs, we produced the nozzle insets via additive manufacturing in stainless steel, using a *ConceptLaser M2* printer.

5.3 Thruster prototype

Fig.6 highlights the main components of entire XMET prototype. The cavity top (yellow) and bottom (gray) parts are CNC machined from stainless steel. The cavity height tuning capability is provided by the thread between these, and leaks are prevented using a K107 type piston seal (a). The Boron Nitride disk (b) is placed into the cavity bottom part and secured with three grub screws (c). Three NPT 1/16" connectors are used for the two propellant ports (d) and a pressure tap port (e) – the latter is connected to an Omega PXM319 pressure transducer. The antenna (f) is machined from copper and screwed to the screw termination of the 7/16 flange-mount coaxial connector jack. Both the observing windows (g) and the nozzle inserts (h) are bolted to the cavity top part and sealed with a standard conflat copper gasket seals (i). The windows are sapphire CF flange type components from LewVac and allow observation of the plasma behaviour during operations. They are mounted next to grids machined into the cavity inner wall, maintaining its required shape for resonance since the hole diameters are small ($\varnothing=1\text{mm}$). Note the cavity height adjustment tuning also changes the size of the annular volume around the dielectric slab, which is part of the internal resonant cavity volume. This was accounted for in the analysis described in Section 4.

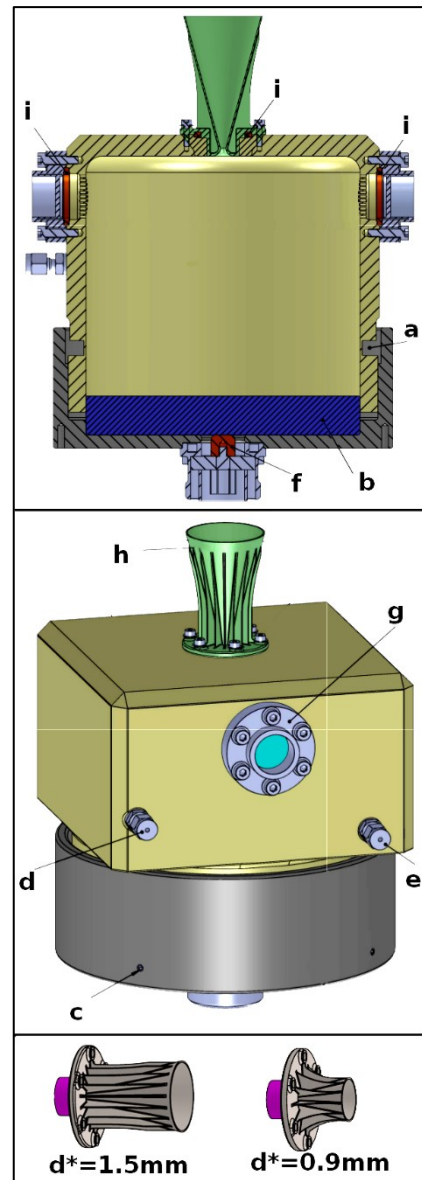


Figure 6: CAD drawings of XMET and two of the nozzle insets with different throat diameters. Labelled parts are described in Section 5.3.

6. CONCLUSION AND OUTLOOK

This work describes the design of a microwave electrothermal thruster operating at 2.45 GHz as part of the IMPULSE all-electric propulsion system. We focussed on optimisation of the cylindrical resonant cavity via multiphysics software, maximising the electric field strength reached at the nozzle throat. We selected Boron Nitride as the dielectric material, avoiding the extremely narrow resonance peak of an optimised design with Alumina. We created a tuneable cavity design for experimental verification of the predicted resonant properties and to allow compensation for machining tolerances and variations in dielectric permittivity. Our XMET prototype uses exchangeable nozzle insets with different throat sizes, which were produced with additive manufacturing.

We are verifying the predicted XMET resonant cavity properties by measuring forward and reflected power as a function of tuneable cavity height, using our microwave generator network. XMET performance is being characterised via direct thrust measurements, by vertically mounting the prototype to a thrust balance inside the 2x4.5m vacuum chamber of the David Fearn Electric Propulsion laboratory at the University of Southampton. Tests are initially using argon to reduce costs before moving to xenon propellant. We will identify the optimum operating regime in terms of pressure and nozzle size that maximises specific impulse at the 200-500 mN thrust level. Performance will be measured at a range of input power levels from 100W up to 1kW.

A future flight-like design will clearly be much simpler than the prototype described in this work, without the need for observing windows, pressure tap, exchangeability of the nozzle and the height tuning configuration. Once the optimised operating pressure has been determined with our current prototype, we will update our FEM stress calculations and create a thin-walled, mass-optimised XMET design that can still withstand the required pressures.

7. ACKNOWLEDGEMENTS

The IMPULSE project is funded by the UK Space Agency's National Space Technology Programme (NSTP3-FT-65).

8. REFERENCES

1. Wells, N., Walker R., Green S. and Ball A. (2006). SIMONE: Interplanetary Microsatellites for NEO Rendezvous Missions, *Acta Astronautica*, 59, 700-709.
2. Clemens, D.E. (2008). Performance Evaluation of the Microwave Electrothermal Thruster Using Nitrogen, Simulated Hydrazine, and Ammonia, PhD Thesis, The Pennsylvania State University.
3. Abaimov, M. D. (2015). Preliminary Testing of a 17.8-GHz Microwave Electrothermal Thruster for Small Spacecraft, Master of Science Thesis, The Pennsylvania State University.
4. Brandenburg, J. E., Kline, J., and Sullivan, D. (2005). The Microwave Electro-Thermal (MET) Thruster Using Water Vapor Propellant, *IEEE Transactions on Plasma Science*. 33:2, 776-782.
5. Yildiz, M.S., Kokal, U. and Celik, M. (2017). Preliminary Thrust Measurement Results of the BUSTLab Microwave Electrothermal Thruster, *53rd Joint Propulsion Conference*, Atlanta, AIAA-2017-4725.
6. Romei, F., Grubisic, A., Gibbon, D., Lane, O., Hertford, R.A. and Roberts, G. (2015). A Thermo-fluidic Model for a Low Power Xenon Resistojet, *34th International Electric Propulsion Conference*, Kobe, IEPC-2015-265.
7. Balaam, P. and Micci, M. M. (1995). Investigation of stabilized resonant cavity microwave plasmas for propulsion, *Journal of Propulsion Power*. 11:5, 1021-1027.
8. Gao, E. and Bilen, S.G. (2008). COMSOL Multiphysics Modeling of a 20W Microwave Electrothermal Thruster, *Proceedings of the 2008 COMSOL Conference*, Boston.
9. Yildiz, M. S., Unaldi, N. and Celik, M. (2014). Geometry Optimization of a 2.45 GHz Microwave Electrothermal Thruster Resonant Cavity, *Space Propulsion Conference*, Cologne, SP2014_2980822.
10. Tondu, T., Chardon, J. and Zurbach, S. (2011). Sputtering yield of potential ceramics for Hall Effect Thruster discharge channel, *32nd International Electric Propulsion Conference*, Wiesbaden, IEPC-2011-106.